AEM Accepted Manuscript Posted Online 3 November 2021
Appl Environ Microbiol doi:10.1128/AEM.01665-21
Copyright © 2021 Rasheedkhan Regina et al.
This is an open-access article distributed under the terms of the Creative Commons Attribution 4.0 International license.

Applied and Environmental Microbiology
AEM
Applied and Environmental Microbiology
Accepted Manuscript Posted Online

1 **Loss of the acetate switch in *Vibrio vulnificus* enhances predation defence against**

2 ***Tetrahymena pyriformis***

3 Viduthalai Rasheedkhan Regina [1,†], Parisa Noorian [2,†], Clarence Sim Bo Wen[1], Florentin

4 Constancias[1], Eganathan Kaliyamoorthy[1], Sean C. Booth[1], Gustavo Espinoza-Vergara[2], Scott

5 A. Rice[1,2,3*] and Diane McDougald[2*]

6 [1] Singapore Centre for Environmental Life Sciences Engineering, Nanyang Technological

7 University, Singapore

8 [2] The iThree Institute, University of Technology Sydney, Sydney, Australia

9 [3] The School of Biological Sciences, Nanyang Technological University, Singapore

10 †These authors contributed equally to this work.

11

12 **†Equal contribution**

13 Viduthalai Rasheedkhan Regina and Parisa Noorian contributed equally to this work. Author

14 order was determined based on taking the lead in writing the manuscript.

15 *** Correspondence:**

16 Diane McDougald email: Diane.McDougald@uts.edu.au

17 Scott A. Rice email: RSCOTT@ntu.edu.sg

18

19 **Keywords:** *V. vulnificus*, protozoan predation, grazing resistance, overflow metabolism,

20 acetate switch, predation defence

21 **Running title: Loss of the acetate switch enables protozoan defence**

22

Downloaded from https://journals.asm.org/journal/aem on 01 December 2021 by 116.255.0.193.

Accepted Manuscript Posted Online
Applied and Environmental Microbiology
AEM
Applied and Environmental Microbiology

23 **Abstract**

24 *Vibrio vulnificus* is an opportunistic human pathogen and autochthonous inhabitant of coastal
25 marine environments, where the bacterium is under constant predation by heterotrophic
26 protists or protozoans. As a result of this selection pressure, genetic variants with anti-
27 predation mechanisms are selected for and persist in the environment. Such natural variants
28 may also be pathogenic to animal or human hosts, making it important to understand these
29 defence mechanisms. To identify anti-predator strategies, thirteen *V. vulnificus* strains of
30 different genotypes isolated from diverse environments were exposed to predation by the
31 ciliated protozoan, *Tetrahymena pyriformis,* and only strain ENV1 was resistant to predation.
32 Further investigation of the cell-free supernatant showed that ENV1 acidifies the
33 environment by the excretion of organic acids, which is toxic to *T. pyriformis*. As this
34 predation resistance was dependent on the availability of iron, transcriptomes of *V. vulnificus*
35 in iron-replete and iron-deplete conditions were compared. This analysis revealed that ENV1
36 ferments pyruvate and the resultant acetyl-CoA leads to acetate synthesis under aerobic
37 conditions, a hallmark of overflow metabolism. The anaerobic respiration global regulator,
38 *arcA*, was upregulated when iron was available. An Δ*arcA* deletion mutant of ENV1
39 accumulated less acetate and importantly, was sensitive to grazing by *T. pyriformis*. Based on
40 the transcriptome response and quantification of metabolites, we conclude that ENV1 has
41 adapted to overflow metabolism and has lost a control switch that shifts metabolism from
42 acetate excretion to acetate assimilation, enabling it to excrete acetate continuously. We show
43 that overflow metabolism and the acetate switch contribute to prey-predator interactions.

44 **Importance**

45 Bacteria in the environment, including *Vibrio* spp., interact with protozoan predators. To
46 defend against predation, bacteria evolve anti-predator mechanisms ranging from changing
47 morphology, biofilm formation and secretion of toxins or virulence factors. Some of these

Downloaded from https://journals.asm.org/journal/aem on 01 December 2021 by 116.255.0.193.

Accepted Manuscript Posted Online

Applied and Environmental Microbiology

AEM

Applied and Environmental Microbiology

48 adaptations may result in strains that are pathogenic to humans. Therefore, it is important to
49 study predator defence strategies of environmental bacteria. *V. vulnificus* thrives in coastal
50 waters and infects humans. Very little is know about the defence mechanisms *V. vulnificus*
51 expresses against predation. Here we show that a *V. vulnificus* strain (ENV1) has rewired the
52 central carbon metabolism enabling the production of excess organic acid that is toxic to the
53 protozoan predator, *T. pyriformis*. This is a previously unknown mechanism of predation
54 defence that protects against protozoan predators.

55 **Introduction**

56 *Vibrio vulnificus* is a Gram-negative, halophilic bacterium that thrives in warm marine and
57 estuarine waters. Despite its environmental origin, the bacterium is associated with
58 opportunistic infections that include gastrointestinal infections caused by ingestion of raw or
59 undercooked seafood as well as wound infections caused by exposure of wounds or broken
60 skin to estuarine or seawater resulting in sepsis (1). *V. vulnificus* is responsible for the highest
61 fatality rate among foodborne pathogens (1, 2), and exhibits considerable genetic and
62 phenotypic variation. An allelic difference in a virulence-correlated gene locus (*vcg*)
63 distinguishes the environmental (e.g. from oysters, clams, shrimp, seawater and sediment) E-
64 genotype strains (*vcgE*) from the clinical genotype strains (*vcgC*) (3, 4). More recent analysis
65 of *V. vulnificus* genomes reveals that there are four major clusters (5) or five lineages (6)of
66 strains. The strain studied here, Env1 belongs to cluster 2, lineage 2. The emergence and
67 persistence of pathogenic strains from the environment is attributed in part, to evolutionary
68 adaptations for protection against predation by protozoans (7-9). Bacteria possess multiple
69 predator defence strategies including extracellular defences to avoid ingestion and
70 intracellular defences that include toxin secretion that are ascribed to the origins of
71 extracellular and intracellular pathogenesis (10).

Downloaded from https://journals.asm.org/journal/aem on 01 December 2021 by 116.255.0.193.

Accepted Manuscript Posted Online

Applied and Environmental Microbiology

AEM

Applied and Environmental Microbiology

72 To avoid predation, bacteria such as *Comomonas acidovorans* (11) and *Flectobacillus* spp.
73 (12) form filaments under predation pressure while *Salmonella* spp. (13) alters surface
74 antigens. Biofilm formation is another common strategy for resisting predation (14). In
75 addition to predator avoidance, some bacteria kill and lyse the predator, which has the
76 additional advantage of providing the pathogen with additional nutrients from dead predators
77 (15). *Vibrio cholerae*, *Vibrio fischeri*, *Janthinobacterium lividum* and *Chromobacterium*
78 *violaceum* are some of the bacteria that excrete extracellular toxic factors to kill the
79 protozoans (16-19). *Escherichia coli* also produces toxins such as Shiga toxin (Stx) that can
80 kill *Tetrahymena thermophila* (20). In *V. cholerae*, the type VI secretion system enables
81 contact killing of the amoeba, *Dictyostelium discoideum* and also affects mammalian
82 macrophages (21-23). The PrtV protein kills the flagellate *Cafeteria roenbergensis* and the
83 ciliate *T. pyriformis* (24). Furthermore, release of reactive oxygen species, quorum sensing-
84 mediated biofilm formation, production of vibrio polysaccharides (VPS) and the chitin-
85 dependent production of ammonia (14, 19, 25, 26) are additional mechanisms *V. cholerae*
86 uses to kill protozoan predators. In contrast, the predator defence mechanisms of *V. vulnificus*
87 are not well studied. One well-known predator defence factor of *V. vulnificus* is the
88 multifunctional-auto processing repeats-in-toxins (MARTX toxins), encoded by the *rtxA1*
89 gene, that causes plasmolysis of amoebae (27). MARTXs kill cells by forming pores in the
90 cell membranes (28). However, with the exception of MARTXs, no other mechanisms for
91 predation resistance in *V. vulnificus* have been characterized.

92 The aim of this study was to identify the grazing defence mechanisms of an environmental
93 strain of *V. vulnificus*, ENV1. By analysing the cell-free supernatants of ENV1,
94 transcriptomic analysis and quantification of the excreted metabolites, we show that ENV1
95 has adapted to overflow metabolism by fermenting pyruvate to acetate, despite the presence
96 of oxygen. Overflow metabolism, coupled with the loss of acetate assimilation creates an

Downloaded from https://journals.asm.org/journal/aem on 01 December 2021 by 116.255.0.193.

Accepted Manuscript Posted Online

Applied and Environmental Microbiology

AEM

Applied and Environmental Microbiology

97 acetic acid rich environment that is toxic to *T. pyriformis*. We propose that overflow
98 metabolism and the acetate switch are a novel anti-predator mechanism of *V. vulnificus*
99 ENV1.

100 **Materials and methods**

101 Strains and growth conditions

102 All *V. vulnificus* strains were kindly provided by J. D. Oliver, UNC Charlotte, Charlotte, NC
103 and Shin-Ichi Miyoshi of Okayama University, Japan. Bacterial strains (Table 1) were
104 routinely grown in Luria-Bertani broth (LB, Difco™, Becton Dickinson, New Jersey, USA)
105 supplemented with 2% NaCl and on agar plates (29) as appropriate, with carbenicillin (100
106 µg ml^{-1}). The iron chelator, 2-2' bipyridyl (BPD) (100 µM) (Sigma-Aldrich, MO, USA), was
107 added to the medium to induce iron limitation. *T. pyriformis,* was routinely passaged in 15 ml
108 peptone-yeast-glucose (PYG) medium (20 g l^{-1} proteose peptone, 1 g l^{-1} yeast extract) added
109 to 1 liter 0.1 × M9 minimal medium (6 g l^{-1} NaH_2PO_4, 3 g l^{-1} K_2PO_4, 0.5 g l^{-1} NaCl, 1 g l^{-1}
110 NH_4Cl) supplemented with 0.1 M sterile-filtered glucose in 25 cm^2 tissue culture flasks with
111 ventilated caps (Sarstedt Inc., Nümbrecht, Germany) and incubated statically at room
112 temperature (RT) for 3 days. To remove the nutrient media and to acclimatize the ciliate to
113 phagotrophic feeding, 500 µl of the *T. pyriformis* culture was added to 20 ml of 0.5 × NSS
114 medium (8.8 g l^{-1} NaCl, 0.735 g l^{-1} Na_2SO_4, 0.04 g l^{-1} $NaHCO_3$, 0.125 g l^{-1} KCl, 0.02 g l^{-1}
115 KBr, 0.935 g l^{-1} $MgCl_2$•6 H_2O, 0.205 g l^{-1} $CaCl_2$•2 H_2O, 0.004 g l^{-1} $SrCl_2$•6 H_2O and 0.004 g
116 l^{-1} H_3BO_3) (30) supplemented with 1% heat-killed *Pseudomonas aeruginosa* PAO1 in a 25
117 cm^2 tissue culture flask and incubated at RT statically for 2 d. The heat-killed bacteria (HKB)
118 were prepared as previously described (18). The health of *T. pyriformis* in each flask was
119 determined by inverted phase contract microscopy. The healthy ciliates are fast swimming
120 and distributed throughout the media. Total numbers of *T. pyriformis* were determined by use
121 of a hemocytometer viewed under bright field light microscopy of three 10 µL aliqouts fixed

Downloaded from https://journals.asm.org/journal/aem on 01 December 2021 by 116.255.0.193.

Accepted Manuscript Posted Online
Applied and Environmental Microbiology
AEM
Applied and Environmental Microbiology

122 with 1% Lugol solution (Sigma) (1:1). Videos and images were recorded under these
123 conditions. *Uronema marinum* (Dujardin 1841) was isolated by Dr Martina Erken in 2011 at
124 the Sydney Institute of Marine Science (SIMS) harbour and kept as a non axenic culture.

125 Quantification of *T. pyriformis* predation of planktonic cells

126 To assess predation of planktonic *V. vulnificus*, 10^6 cells ml^{-1} of overnight cultures in 0.5 ×
127 VNSS (1 g bacteriological peptone, 0.5 g yeast extract, 0.5 g D-glucose, 0.01 g $FeSO_4•7H_2O$
128 and 0.01 g Na_2HPO_4 in 1 liter of 0.5 × NSS) (31) were added to 24-well microtiter plates (BD
129 Falcon™, Becton Dickinson, New Jersey, USA). *T. pyriformis* was subsequently added to
130 each well (10^4 cell ml^{-1}; determined by microscopy) and the plates were incubated at RT with
131 shaking at 60 rpm for 24 h. The cell density of each well was measured at $OD_{600\ nm}$
132 (Eppendorf® PlateReader AF2200, Hamburg, Germany). Planktonic fractions were collected
133 for CFU ml^{-1} counts. *T. pyriformis* was enumerated by microscopy.

134 Supernatant toxicity assay

135 To determine if factors secreted by *V. vulnificus* ENV1 were toxic to protozoa, overnight
136 cultures of *V. vulnificus* ENV1 were adjusted to 10^6 cells ml^{-1} in 0.5 × VNSS and incubated
137 for 24 h. Cell-free supernatants (CFS) were collected by centrifugation at 3100 × *g* for 5 min
138 and filtered (0.22 μm, Millipore; Bedford, MA, USA). Various treatments of the CFSs,
139 including heating (95°C for 2 h), freezing/thawing (-20°C for 24 h), ultrafiltration (Amicon®
140 Ultra-0.5-10, 000NMWL), proteinase K (200 μg ml^{-1}) from *Tritirachium album* (Sigma-
141 Aldrich, MO, USA), proteinase (1 mg ml^{-1}) from *Streptomyces griseus* (Pronase E) (Sigma-
142 Aldrich, MO, USA), pH adjustment with hydrochloric acid (HCL, 1-3 mM) and sodium
143 hydroxide (NaOH 1-3 mM) were tested to assess what types of biomolecules may be
144 responsible for toxicity. The CFS was added to 24-well microtiter plates (BD Falcon™,
145 Becton Dickinson, New Jersey, USA) containing *T. pyriformis* (10^4 cell ml^{-1}) and numbers of
146 live *T. pyriformis* were determined by microscopy. Sterile medium controls (0.5 × VNSS)

Downloaded from https://journals.asm.org/journal/aem on 01 December 2021 by 116.255.0.193.

Accepted Manuscript Posted Online

Applied and Environmental Microbiology

AEM

Applied and Environmental Microbiology

147 were included for each treatment to ensure none of the treatments were toxic to *T. pyriformis*.
148 Images of the whole field of view at different time points were taken using inverted phase
149 contrast microscopy. Cells that die due to cytotoxity lose their shape, become more spherical
150 and leak cytoplasm through compromised cell membranes. These cells sink to the bottom of
151 the well. Hence only misshapen, disintegrating cells at the bottom of the well were counted as
152 dead.

153 Estimation of fatty acid content

154 For the estimation of short chain fatty acids (acetate, propionate, butyrate, and valerate), CFS
155 was collected as described previously. CFS was acidified with formic acid (0.1% final
156 concentration) and analysed by GC-FID using a DB-FFAP column (Agilent) with standards
157 of each fatty acid prepared in water at concentrations between 1 and 200 parts per million.

158 RNA extraction and sequencing

159 Overnight cultures of *V. vulnificus* were adjusted to 10^6 cells ml^{-1} ($OD_{600\ nm}$ = 0.001) in 0.5 ×
160 VNSS (iron-replete) or 0.5 × VNSS supplemented with 100 µM of the iron chelator, 2-2'
161 dipyridyl (iron-depleted) in 24-well microtiter plates (BD Falcon™, Becton Dickinson, New
162 Jersey, USA). Plates were incubated for 10 h at RT with shaking at 60 rpm (early stationary
163 phase) and the supernatant toxicity was determined. The samples were fixed in RNAprotect
164 Bacteria Reagent (QIAGEN®). Total RNA was extracted by lysozyme digestion and the
165 RNeasy® Plus Mini kit (QIAGEN®) following the manufacturer's instructions. RNA
166 concentration and purity were determined by spectrophotometer (NanoDrop ND-1000) and
167 the integrity of the RNA was determined by agarose gel electrophoresis and using an Agilent
168 Bioanalyzer 2100. The RNA was stored at -80°C until it was prepared for sequencing using
169 the Illumina standard kit following manufacturer's protocol (Illumina). Samples were
170 sequenced by paired-end sequencing on the Illumina Hi-Seq 2500 platform with read lengths
171 of 100 bp.

Downloaded from https://journals.asm.org/journal/aem on 01 December 2021 by 116.255.0.193.

Accepted Manuscript Posted Online
Applied and Environmental Microbiology
AEM
Applied and Environmental Microbiology

172 Transcriptome data analysis

173 The quality of the paired-end reads was initially checked using FastQC
174 (http://www.bioinformatics.bbsrc.ac.uk/projects/fastqc). Illumina adaptors, short and low-
175 quality reads were removed using cutadapt (version 1.11) (32). In silico rRNA depletion for
176 high-quality reads (97% to 98% of the raw reads) was performed using sortmeRNA (version
177 2.0) (33). Messenger RNA reads (from 75,495 to 131,958 read pairs) were then mapped to
178 the *V. vulnificus* ENV1 genome (34) using Bowtie2 (version 2.2.9) (35). The number of reads
179 mapping to each gene was determined using HTSeq (version v.0.6.1p1) (36).

180 The raw count table of transcripts was then used as an input for the Deseq2 R package for
181 differential expression analysis (37). Briefly, the raw counts were normalized according to
182 sample library size and a negative binomial test was performed to identify the differentially
183 expressed genes. Genes were considered as differentially expressed if their absolute fold-
184 change value was greater than 2 and the associated adjusted p-value was smaller than 0.05.
185 The normalized transcripts were then $\log_2$ (N+1) transformed prior to principal component
186 analysis and UPGMA hierarchical clustering for the sample dendrogram on the heatmap.

187 Generation of *arcA* null mutation

188 A four-fragment construct was generated using NEBuilder HiFi DNA assembly master mix
189 (New England Biolabs), consisting of a 750 bp region upstream of the *arcA* start codon, a
190 750 bp region downstream of *arcA,* a gentamicin resistance cassette and the linearized
191 suicide vector pCVD442 (Addgene #11074). The assembled construct was transformed into
192 *E. coli* BW20767 via heat-shock transformation. The correct insertion of fragments in
193 pCVD442 was confirmed by sequencing (Sanger sequening, 1st Base, Asia).

194 The construct was introduced into *V. vulnificus* ENV1 using electroporation (38).
195 Electrocompetent cells were produced by washing mid-log phase ENV1 cells with 400 mM

Downloaded from https://journals.asm.org/journal/aem on 01 December 2021 by 116.255.0.193.

Accepted Manuscript Posted Online
Applied and Environmental Microbiology
AEM
Applied and Environmental Microbiology

196 sucrose at RT. After electroporation (10 kV/cm, 25 µF, 200 Ω), cells were recovered in SOC
197 supplemented with 2% NaCl for 3 h at 37°C. The *arcA* mutant cells were selected using
198 ABTC medium supplemented with 60 µg ml^{-1} gentamicin at 30°C for 96 h. ABTC medium
199 consists of solutions A and B of the defined growth medium described by Clark and Maaløe
200 (39) supplemented with 2.5 mg L^{-1} thiamine (T) and 10 mM citrate (C). Counter selection of
201 the clones, was achieved by spreading mid-log phase cultures of the 1st recombination clones
202 on counter selection agar containing sucrose (10 g L^{-1} peptone, 5 g L^{-1} yeast extract, 2 g L^{-1}
203 sodium chloride, gentamicin 60 µg ml^{-1} and 15% v/v sucrose). The deletion was confirmed
204 by PCR and sequencing of the PCR product (Sanger sequencing, 1st Base, Asia).

205 Data analysis

206 Statistical analyses were performed using GraphPad Prism version 7.03 for Windows,
207 (GraphPad Software, La Jolla California USA) (www.graphpad.com). Data that did not
208 follow Gaussian distribution, as determined by frequency distribution graphs, were natural
209 log transformed. Two-tailed student's t-tests were used to compare means between
210 experimental samples and controls. For experiments including multiple samples, one-way or
211 2-way ANOVAs were used for the analysis and Sidak's or Dunnett's multiple comparison test
212 provided post-hoc comparison of means when appropriate.

213 **Results**

214 *V. vulnificus* ENV1 is resistant to *T. pyriformis* predation

215 Thirteen strains of *V. vulnificus*, representing different genotypes and isolation sources (Table
216 1), were assessed for grazing resistance against *T. pyriformis*. Twelve strains showed
217 significant reduction in bacterial biomass compared to the bacteria grown alone (Figure 1A)
218 and the number of *T. pyriformis* also increased significantly when compared to growth
219 without bacteria (VNSS control) (Figure 1B). In contrast, the biomass of strain ENV1 was
220 not reduced by *T. pyriformis* predation (Figure 1A) and the number of *T. pyriformis* cells was

Downloaded from https://journals.asm.org/journal/aem on 01 December 2021 by 116.255.0.193.

Accepted Manuscript Posted Online

Applied and Environmental Microbiology

AEM

Applied and Environmental Microbiology

221 not significantly different to the control (Figure 1B). This suggests that, in contrast to the
222 other twelve strains, ENV1 defended against predation by *T. pyriformis*. The toxicity of
223 ENV1 CFS was also tested on the salt-water ciliate, *U. marinum*. The addition of ENV1 CFS
224 caused the same cell death observed in *T. pyriformis* after less than 5 minutes (data not
225 shown).

226 *V. vulnificus* ENV1 excretes a pH sensitive, toxic-factor in the presence of iron

227 To determine if ENV1 defence was based on secreted factors, *T. pyriformis* was incubated
228 with the CFS of ENV1 grown for 24 h in 0.5 × VNSS medium. After 10 min at RT, the
229 ciliates stopped swimming and sank to the bottom of the microtiter plates. After 1 h, the
230 ciliates were dead (100 %) with their cytoplasm leaking out (Figure 2B). After 2 h, the ciliate
231 cells were observed to be degraded (Figure 2C). In contrast, *T. pyriformis* incubated in VNSS
232 without CFS remained healthy throughout the experiment (Figure 2A). This effect of the
233 ENV1 CFS on *T. pyriformis* suggested that the bacteria excrete toxic factors that can
234 permeabilize and degrade the cell membrane of *T. pyriformis* leading to cell death.

235 *V. vulnificus* is a ferrophilic bacterium that requires high levels of iron for pathogenicity (40).
236 Therefore, the role of iron in grazing resistance was evaluated by assessing the toxicity of
237 CFS of ENV1 grown under iron-depleted conditions (by supplementing the 0.5 × VNSS with
238 2-2' bipyridyl). The CFS produced under iron-depleted conditions was unable to kill *T.*
239 *pyriformis* (Table 2). The iron limitation enabled grazing on ENV1 (Figure 3A) and the
240 number of *T. pyriformis* doubled (Figure 3B). The loss of toxicity towards *T. pyriformis*, and
241 the loss of grazing resistance of ENV1 when grown under iron-depleted conditions strongly
242 suggests that excretion of the toxic factor by ENV1 is linked to iron-dependent metabolism.

243 The toxicity of the CFS after physical and chemical treatments was also determined (Table
244 2). Heating at 95°C for 2 h, freezing at -20°C and thawing, or proteases (pronase-E and

Downloaded from https://journals.asm.org/journal/aem on 01 December 2021 by 116.255.0.193.

Accepted Manuscript Posted Online
Applied and Environmental Microbiology
AEM
Applied and Environmental Microbiology

245 proteinase K) treatments did not affect the CFS toxicity against *T. pyriformis*. Furthermore,
246 ultrafiltration through 0.5 - 10,000 NMWL filters did not alter CFS toxcity, suggesting the
247 secreted factor was likely smaller than 10 kDa. Collectively, the results indicate that the toxic
248 factor is not an enzyme or a protein. The CFS pH was approximately 4 and therefore, the role
249 of pH in toxicity was examined. Neutralization of the pH to 7 using sodium hydroxide
250 rendered the CFS non-toxic to *T. pyriformis* (Table 2). Furthermore, to validate if acidity kills
251 *T. pyriformis*, the pH of sterile VNSS medium was adjusted to below 4.6 using hydrochloric
252 acid. This acidified VNSS did not affect the viability of *T. pyriformis*, confirming that the
253 toxicity was not because of the acidity, but a toxic factor that is sensitive to pH differences
254 (Table 2).

255 *V. vulnificus* ENV1 kills *T. pyriformis* by excreting acetic acid

256 The CFS analysis indicated that the toxic factor is not an enzyme or a protein (heat treatment)
257 and thus, is likely a small molecule (ultrafiltration) and that its function is affected by
258 protonation of functional groups (active in acidic pH). Free fatty acids are small organic
259 compounds produced by several bacteria that have antimicrobial properties, which are
260 dependent on the pH of the environment (41). Therefore, the CFS was tested for the presence
261 of the short-chain fatty acids (SCFAs) acetate, propionate, butyrate and valerate using gas
262 chromatography. The CFS contained approximately 4 mM acetate, while the other SCFAs
263 could not be detected (Figure 3C). Addition of acetic acid to sterile VNSS made the medium
264 acidic depending on the concentration of the fatty acid. The medium supplemented with 1
265 and 2 mM acetic acid changed the pH of the media to 5.5 and 4.8, respectively, but was non-
266 toxic to *T. pyriformis*. However, 3 mM acetic acid resulted in a pH of 3.8 and killed the
267 ciliates (Table 2). Furthermore, adjusting the pH of the medium containing 1 and 2 mM
268 acetic acid to approximately 4 rendered the medium toxic to *T. pyriformis* (Table 2). These

Downloaded from https://journals.asm.org/journal/aem on 01 December 2021 by 116.255.0.193.

Accepted Manuscript Posted Online

Applied and Environmental Microbiology

AEM

Applied and Environmental Microbiology

269 results suggest that the toxic factor excreted by the strain ENV1 is acetic acid and that it is
270 active against *T. pyriformis* in its protonated form (acetic acid pKa = 4.6), under acidic pH.

271 The CFS was only toxic to *T. pyriformis* when ENV1 grew in the presence of iron (Figure
272 3A, 3B) and in the absence iron, the concentration of acetate was significantly less than that
273 of iron-replete conditions (Figure 3C, D). The growth of ENV1 without iron was unaffected
274 (Figure 3E) and change in pH of the iron-depleted CFS was significantly slower (relatively
275 alkaline) than for the WT (Figure 3F). The low concentration of acetate in the CFS during
276 iron-depletion suggests that acetate excretion of ENV1 is dependent on iron.

277 *V. vulnificus* ENV1 excretes excess acetic acid through overflow metabolism

278 To understand the iron-dependent mechanism of acetate excretion in ENV1, the
279 transcriptomes of ENV1 cultures grown under iron-replete and iron-depleted conditions were
280 analysed by RNA sequencing (Table 3, Table S1).

281 Acetate excretion in Gammaproteobacteria such as *Vibrio* spp. and *E. coli*, follows two
282 different pathways: 1) by direct oxidation of pyruvate by pyruvate oxidase (PoxB) and 2) by
283 decarboxylation of pyruvate to acetyl-CoA, followed by the conversion of acetyl-CoA to
284 acetate by phosphotransacetylase (Pta) and acetate kinase (AckA). Decarboxylation of
285 pyruvate to acetyl-CoA can occur both aerobically, by pyruvate dehydrogenase complex
286 (PdhC) and anaerobically by pyruvate-formate lyase (Pfl) (42). *V. vulnificus* strains lack *poxB*
287 and therefore direct oxidation of pyruvate to acetate is not possible. Under iron-replete
288 conditions, *pdhC* (BJD94_14015) was downregulated and *pfl* genes (BJD94_01215 and
289 BJD94_08715) were upregulated (Table 3, Table S1), suggesting that the pyruvate is
290 converted to acetyl-CoA by fermentation. Furthermore, ENV1 encodes two copies of *ackA*
291 genes (BJD94_01780 and BJD94_2925), both of which were upregulated under iron-replete
292 conditions. This indicates that conversion of acetyl-CoA to acetate follows the Pta-AckA

Downloaded from https://journals.asm.org/journal/aem on 01 December 2021 by 116.255.0.193.

Accepted Manuscript Posted Online
Applied and Environmental Microbiology
AEM
Applied and Environmental Microbiology

293 pathway and suggests that ENV1 is adapted for acetate excretion through pyruvate
294 fermentation. Moreover, the upregulation of genes associated with alcohol/acetaldehyde
295 dehydrogenase (*adh/aldH*) (BJD94_06220) suggested that acetate accumulates through
296 conversion of acetyl-CoA to ethanol and acetaldehyde and contributes to replenishing NAD^+
297 from NADH. In addition to decarboxylation of pyruvate, Pfl also catalyzes pyruvate to
298 formate, which is a metabolic intermediate that also helps replenish the NAD^+ pool.
299 Furthermore, *fdhA* (BJD94_18845, formate dehydrogenase) that converts formate to carbon
300 dioxide was also upregulated under the iron-replete conditions (Table 3).

301 Acetate excretion through the Pta-AckA pathway in *E. coli* (42) as well as in *V. cholerae* (43)
302 is associated with the suppression of TCA cycle enzymes by the anaerobic respiration control
303 protein, ArcA (BJD94_08750), which was upregulated under iron-replete conditions (Table
304 3). Together with the upregulation of *ackA*, *pfl*, adh/aldh and *fdhA*, and the downregulation of
305 *pdhC*, the transcriptome data suggested that ENV1 generates ATP primarily by excreting
306 acetate (*pfl*, *ackA*) and regenerates NAD^+ by excreting partially oxidized intermediates such
307 as ethanol and formate (*adh*, *pfl*) through pyruvate fermentation (Figure 4). These phenotypes
308 are characteristic of anaerobic growth despite the experiments being conducted under aerobic
309 conditions. Env1 grew at a faster rate during the first 3 h and did not appear to grow further
310 (Figure 3E, 5B), which is a characteristic growth pattern for overflow metabolism (42).
311 Several microorganisms use overflow metabolism when carbon flux through glycolysis is
312 higher than for the tricarboxylic acid (TCA) cycle, resulting in the fermentation of pyruvate
313 to acetate for energy generation instead of respiration, despite the presence of oxygen.
314 Transcriptome analysis indicated that ENV1 was actively expressing genes associated with
315 the glycolysis pathway and had repressed TCA cycle genes. This was based on the
316 upregulation of both *arcA* and fermentation pathway genes involved in conversion of
317 pyruvate to acetate (Figure 4, Table 3). The above phenotype was confirmed by estimation of

Downloaded from https://journals.asm.org/journal/aem on 01 December 2021 by 116.255.0.193.

Accepted Manuscript Posted Online

Applied and Environmental Microbiology

AEM

Applied and Environmental Microbiology

318 acetate in the CFS (Figure 3C, 3D, 5A), which strongly suggested that *V. vulnificus* ENV1
319 has adapted to overflow metabolism.

320 <u>Acetate excretion is controlled by the anaerobic respiration control protein, ArcA</u>

321 To determine if *arcA* controls acetate excretion, and hence predation defence, in ENV1, *arcA*
322 was deleted. The *ΔarcA* mutant was more grazing sensitive compared to the WT and the
323 number of predators also increased significantly compared to that of WT ENV1 (Figure 3A,
324 3B). Deletion of *arcA* did not affect the growth of the mutant, but the acetate concentrations
325 in the CFS of *ΔarcA* was significantly lower than the WT, suggesting that a slower acetate
326 excretion rate is linked to the grazing sensitivity of the mutant ENV1 (Figure 3A, D, E).
327 Therefore, it is clear that *arcA* influences predator defence by controlling the rate of acetate
328 excretion of ENV1.

329 <u>Loss of the acetate-switch leads to excess acetate accumulation by ENV1</u>

330 The acetate-switch is a phenomenon when cells switch from acetate excretion through
331 overflow metabolism to assimilation through the Pta-AckA or the PoxB (if present)
332 pathways. For example, a grazing sensitive *V. vulnificus* strain (L180) initially excreted
333 acetate but switched to assimilation after 3 h (Figure 5A). In contrast, ENV1 continued to
334 excrete acetate without subsequent re-assimilation over 24 h, suggesting that acetate switch
335 phenomenon is absent in ENV1. Furthermore, L180 had an initial lag phase followed by
336 exponential growth, whereas ENV1 grew faster initially and had no observable lag phase
337 (Figure 5B). In support of the excess acetate excretion, ENV1 acidified the medium
338 immediately, while L180 showed a slight increase in pH (Figure 5C). The difference in
339 growth phases and medium acidification indicate a fundamental difference in metabolism.
340 The ability to produce higher concentrations of acetate and the lack of its assimilation, when
341 compared to that of L180 (Figure 5), suggested that ENV1 lacked the acetate-switch and has
342 adapted to survive primarily through overflow metabolism.

Downloaded from https://journals.asm.org/journal/aem on 01 December 2021 by 116.255.0.193.

Accepted Manuscript Posted Online

Applied and Environmental Microbiology

AEM

Applied and Environmental Microbiology

343 **Discussion**

344 Mechanism of predation resistance

345 We tested 13 different *V. vulnificus* strains, representing different genotypes and isolation
346 sources, for resistance to predation by *T. pyriformis.* Only ENV1 showed resistance to
347 predation by *T. pyriformis* (Figure 1A). Furthermore, co-incubation with ENV1 resulted in
348 growth inhibition and toxicity to *T. pyriformis* (Figure 1B, 2). This toxicity was also observed
349 for the CFS of ENV1 (Table 2).

350 Acetate is secreted and acts as a predation defence for ENV1

351 The CFS of ENV1, when subjected to ultrafiltration, protease treatment or heating and
352 freezing was toxic to *T. pyriformis*. However, neutralizing the original pH (approximately 4)
353 by adding NaOH rendered the CFS non-toxic, indicating that active ingredient that confers
354 toxicity is less likely to be a protein or enzyme, but a small compound that is sensitive to pH,
355 such as organic acids. High concentrations of acetate (up to 4 mM) were detected in the CFS
356 of ENV1 (Figure 3C, 5A), while no other SCFA could be detected (Figure 3C). Furthermore,
357 when acetate was added to the fresh medium and the pH of the medium is less than its pKa
358 (4.6), *T. pyriformis* was killed (Table 2).

359 SCFAs are weak acids, and when the carboxylic group is protonated, can diffuse across cell
360 membranes and dissociate releasing H^+ ions in the cells. Intracellar protonated SCFAs
361 contribute to increases in hydrogen ion concentrations resulting in an unfavourable
362 intracellular pH leading to compromised cellular function (44-46). *T. pyriformis* growth is
363 sensitive to changes in intracellular pH. For example, nigericin, an antibiotic derived from
364 *Streptomyces* spp., is a carboxylic polyether compound that acts as an ionophore and an
365 antiporter of H^+ and K^+ ions. Treatment with nigericin results in an acidified intracellular
366 environment for *T. pyriformis* (47, 48) and is hence toxic. Additionally, weak acids can
367 perturb cell membranes through disruption of electron transport chains, interfering with

Downloaded from https://journals.asm.org/journal/aem on 01 December 2021 by 116.255.0.193.

Accepted Manuscript Posted Online

Applied and Environmental Microbiology

AEM

Applied and Environmental Microbiology

368 oxidative phosphorylation leading to compromised ATP synthesis, form peroxides or auto-
369 oxidation products leading to free radical generation and membrane lysis (49, 50). Treatment
370 of *T. pyriformis* with ENV1 CFS or the VNSS medium supplemented with acetic acid, led to
371 leakage of the cytoplasm out of the cell membrane (Figure 2). Collectively, the data suggest
372 that acetate secretion by *V. vulnificus* ENV1 is the mechanism of grazing resistance against *T.*
373 *pyriformis*.

374 *V. vulnificus* is ferrophilic and iron plays a key role in pathogenicity(40, 51). The CFS from
375 cells grown under iron depleted conditions contained significantly less acetate and were no
376 longer toxic to *T. pyriformis* (Figure 3D, Table 2). In addition, the pH of the culture medium
377 was above the pKa of acetic acid when grown under iron-depleted conditions (Table 2). The
378 change in toxicity, acetate concentration, and the pH indicate that iron plays a key role in the
379 acetate excretion and the acidification of the environment and so the defence of ENV1
380 against *T. pyriformis*.

381 Acetate excretion

382 Acetogenesis, the excretion of acetate, generates energy and recycles coenzyme A. Acetate
383 excretion occurs either by direct oxidation of pyruvate catalyzed by pyruvate oxidase (PoxB)
384 under aerobic conditions, or by decarboxylation of pyruvate (under both aerobic and
385 anaerobic conditions) to acetyl-CoA followed by generation of acetyl-phosphate then acetate,
386 catalyzed by phosphotrasacetylase (Pta) and acetyl kinase (AckA). ENV1, like most *Vibrio*
387 spp. lacks *poxB* and likely decarboxylates pyruvate to acetyl-CoA and converts it to acetate
388 through the Pta-AckA pathway. Decarboxylation of pyruvate to acetyl-CoA can occur both
389 aerobically by pyruvate dehydrogenase complex (PdhC), and anaerobically by pyruvate-
390 formate lyase (Pfl) (42). ENV1 encodes both enzymes, as well as *pta* and *ackA* genes in
391 chromosome one and a second copy of *ackA* in chromosome two (34). Transcriptomic
392 analysis of ENV1 grown under iron-replete compared to iron-depleted conditions showed

Downloaded from https://journals.asm.org/journal/aem on 01 December 2021 by 116.255.0.193.

Accepted Manuscript Posted Online

Applied and Environmental Microbiology

AEM

Applied and Environmental Microbiology

393 that *pdhC* was repressed, while *pfl* was induced, suggesting decarboxylation of pyruvate to
394 acetyl-CoA without the need for oxygen. Furthermore, both copies of *ackA* were upregulated
395 in the presence of iron, confirming the involvement of the Pta-AckA pathway in the
396 conversion of acetyl-CoA to acetate (Table 3).

397 In *E. coli*, anaerobic respiration is regulated by ArcA that represses TCA cycle genes (52,
398 53). ArcA is also involved in regulating overflow metabolism, where cells enter a
399 fermentative growth phase despite the presence of oxygen resulting in faster growth but with
400 deceased ATP production per molecule of glucose. TCA cycle enzymes are repressed by
401 ArcA expression diverting the carbon flux towards the excretion of acetate to generate energy
402 (54-56). Here, *arcA* was upregulated in ENV1 under iron-replete conditions and the
403 transcripts of TCA cycle genes were not upregulated, indicating that the strain carries out
404 overflow metabolism for energy generation (Figure 4, Table 3). The higher acetate
405 concentration (Figure 3D, 5A) in the CFS and the faster growth rate (Figure 3E, 5B) also
406 confirmed that ENV1 was undergoing over flow metabolism. The *ΔarcA* mutant produced
407 less acetate (Figure 3D) and was sensitive to *T. pyriformis* grazing (Figure 3A), confirming
408 that the acetate excretion was dependent on *arcA*.

409 While acetate excretion contributes to ATP generation, cells also require NAD^+ to maintain
410 glycolysis that generates pyruvate from glucose. However, during glycolysis, 2 molecules of
411 NADH are produced for each molecule of glucose oxidized, depleting NAD^+, which is a
412 substrate for the glycolytic enzyme glyceraldehyde-3-phosphate dehydrogenase. Therefore,
413 cells need to replenish the NAD^+ pool to maintain the glycolytic flux and this can be
414 achieved by reoxidation of NADH mediated by the excretion of partially oxidized metabolic
415 intermediates such as lactate, formate and ethanol in the absence of the TCA cycle. While
416 lactate dehydrogenase (*ldh*), the enzyme responsible for lactate synthesis, was not
417 significantly upregulated, lactate as well as formate were detected at mM concentrations in

Downloaded from https://journals.asm.org/journal/aem on 01 December 2021 by 116.255.0.193.

Accepted Manuscript Posted Online

Applied and Environmental Microbiology

AEM

Applied and Environmental Microbiology

418 the CFS of ENV1 (Figure S1). Furthermore, genes responsible for the synthesis of formate
419 (*pfl*) and ethanol (*adh*) were induced (Table 3). Thus, it is evident that *V. vulnificus* ENV1 is
420 adapted for oxygen-independent overflow metabolism.

421 The missing acetate switch

422 Many bacteria excrete acetate when an acetogeniec substrate is available and then re-
423 assimilate the excreted acetate when the extracellular concentrations of the acetate are high
424 and the substrate low. This phenomenon of switching from excretion to assimilation is called
425 the 'acetate switch' (42). When we measured the acetate concentration of ENV1 and the
426 grazing sensitive strain L180, we found that strain L180 was able to excrete acetate and then
427 switch to assimilation when the extracellular concentration of acetate was around 1 mM and
428 did not excrete more acetate over 24 h of growth (Figure 5A). In contrast, ENV1 continued to
429 excrete acetate without assimilating it over the 24 h of growth under aerobic conditions. This
430 lack of acetate assimilation shows that ENV1 has adapted mechanisms to not to switch to
431 acetate assimilation, but continues to produce acetate, which results in an acidic environment.
432 The lack of this acetate switch can happen through at least three different routes, which may
433 also be interconnected, 1) maintaining *arcA* expression and activation 2) modulation of the
434 cAMP and NAD^+ pool required for the transcription and activation of acetyl-CoA synthase
435 (57) and 3) quorum-sensing mediated switching(57, 58). Further studies are required to
436 understand how ENV1 has acquired this adaptation.

437 It has been suggested that the evolution of emergent pathogens as well as their persistence in
438 the environment is in part due to selection pressures associated with predation and the
439 development of various mechanisms of predation resistance (7-9). Resistance to protozoan
440 grazing mediated by the oxygen independent overflow metabolism in the absence of acetate
441 switch is a previously unknown mechanism of predation defence. While the implication for
442 such an adaptation to pathogenesis in Env1 is unknown, anaerobic respiration has been

Downloaded from https://journals.asm.org/journal/aem on 01 December 2021 by 116.255.0.193.

Accepted Manuscript Posted Online
Applied and Environmental Microbiology
AEM
Applied and Environmental Microbiology

443 shown to induce virulence factor production in other *Vibrio spp*. (43, 59). For example, a
444 transposon insertion mutation in the primary respiration-linked sodium pump (Na^{+}NQR)
445 resulted in hypoxic growth in *V. cholerae* that led to increased transcription of the virulence
446 gene regulator *toxT* that in turn induces the production of the cholera toxin. Furthermore,
447 *arcA* expression-linked repression of TCA cycle and increased acetate excretion are also
448 associated with increased *toxT* transcription (43). Env1 does not encode *toxT* and
449 transcription of no known toxic genes were observed in this study. However, given that
450 overflow acetate metabolism of ENV1 is a natural variation of the central carbon metabolism
451 that exists in the environment, it is likely that *V. cholerae*, like other potential pathogens can
452 acquire such metabolic adaptation in their natural habitat. It is not clear if *V. vulnificus*
453 ENV1, which was isolated from an oyster, has adapted to the unique combination of
454 overflow metabolism and the lack of acetate switch as a result of interactions with protozoan
455 predators. However, the discovery of such a strain from the natural environment presents a
456 compelling case for active environmental surveillance for natural variants that might emerge
457 as potential human pathogens.

458 **Conclusions**

459 In conclusion, we found that *V. vulnificus* ENV1 was resistant to predation by *T. pyriformis*.
460 ENV1 has adapted to overflow metabolism, where it ferments pyruvate and generates energy
461 by excreting acetate under aerobic conditions. ArcA, the anaerobic response regulator, plays
462 a key role in the acetate excretion of ENV1, and therefore is indirectly involved in predator
463 defence. Furthermore, the adaptation involves the loss of the ability to assimilate excreted
464 acetate (the acetate switch) and as a result the excreted acetate and other organic acids
465 acidifies the environment. Therfore, acetate excretion under an acidified environment is a
466 novel bacterial anti-predator stratergy that provides protection for *V. vulnificus* ENV1..

467 **Acknowledgements**

Downloaded from https://journals.asm.org/journal/aem on 01 December 2021 by 116.255.0.193.

Accepted Manuscript Posted Online
Applied and Environmental Microbiology
AEM
Applied and Environmental Microbiology

468 The authors would like to acknowledge support from the iThree Institute at the University of
469 Technology Sydney, Sydney, Australia, the Australian Research Council Discovery Project
470 (DP170100453) and by the National Research Foundation and Ministry of Education
471 Singapore under its Research Centre of Excellence Program to the Singapore Centre for
472 Environmental Life Sciences Engineering, Nanyang Technological University.

473 **Conflict of Interest**

474 The authors declare that the research was conducted in the absence of any commercial or
475 financial relationships that could be construed as a potential conflict of interest.

476 **Author Contributions**

477 VRR, PN, GE, SAR and DM conceptualized the overall reasearch. VRR, PN and FC did data
478 curation and formal analysis. VRR, PN, CSBW, FC, EK, SCB and GE took part in the
479 investigation. VRR, PN, CSBW and SCB were involved in the methadology development.
480 SAR and DM took care of funding acquisition, project administration, providing research
481 resources, supervision and validation of the research. VRR and PN did the visualization and
482 presentation of the data. VRR took the lead in writing the manuscript with significant
483 contribution from PN. All authors provided critical feedback and helped shape the research,
484 analysis and manuscript review and editing.

485

Downloaded from https://journals.asm.org/journal/aem on 01 December 2021 by 116.255.0.193.

Accepted Manuscript Posted Online
Applied and Environmental Microbiology
AEM
Applied and Environmental Microbiology

486 **References**

487 1. Oliver JD. 2013. *Vibrio vulnificus*: death on the half shell. A personal journey with
488 the pathogen and its ecology. Microb Ecol 65:793-9.
489 2. Horseman MA, Surani S. 2011. A comprehensive review of *Vibrio vulnificus:* an
490 important cause of severe sepsis and skin and soft-tissue infection. Int J Infect Dis
491 15:e157-66.
492 3. Rosche TM, Yano Y, Oliver JD. 2005. A rapid and simple PCR analysis indicates
493 there are two subgroups of *Vibrio vulnificus* which correlate with clinical or
494 environmental isolation. Microbiol Immunol 49:381-389.
495 4. Warner EB, Oliver JD. 2008. Multiplex PCR assay for detection and simultaneous
496 differentiation of genotypes of *Vibrio vulnificus* biotype 1. Foodborne Pathog Dis
497 5:691-3.
498 5. López-Pérez M, Jayakumar JM, Haro-Moreno JM, Zaragoza-Solas A, Reddi G,
499 Rodriguez-Valera F, Shapiro OH, Alam M, Almagro-Moreno S, Laub MT, Jensen P,
500 Gómez-Consarnau L. 2019. Evolutionary Model of Cluster Divergence of the
501 Emergent Marine Pathogen *Vibrio vulnificus*: From Genotype to Ecotype. mBio
502 10:e02852-18.
503 6. Roig FJ, González-Candelas F, Sanjuán E, Fouz B, Feil EJ, Llorens C, Baker-Austin
504 C, Oliver JD, Danin-Poleg Y, Gibas CJ, Kashi Y, Gulig PA, Morrison SS, Amaro C.
505 2018. Phylogeny of *Vibrio vulnificus* from the Analysis of the Core-Genome:
506 Implications for Intra-Species Taxonomy. Front Microbiol 8.
507 7. Sun S, Noorian P, McDougald D. 2018. Dual Role of Mechanisms Involved in
508 Resistance to Predation by Protozoa and Virulence to Humans. Front Microbiol
509 9:1017.

Downloaded from https://journals.asm.org/journal/aem on 01 December 2021 by 116.255.0.193.

Accepted Manuscript Posted Online
Applied and Environmental Microbiology
AEM
Applied and Environmental Microbiology

510 8. Espinoza-Vergara G, Hoque MM, McDougald D, Noorian P. 2020. The Impact of
511 Protozoan Predation on the Pathogenicity of *Vibrio cholerae*. Front Microbiol 11:17.
512 9. Jones MK, Oliver JD. 2009. *Vibrio vulnificus*: disease and pathogenesis. Infect
513 Immun 77:1723-33.
514 10. Matz C, Kjelleberg S. 2005. Off the hook–how bacteria survive protozoan grazing.
515 Trends Microbiol 13:302-307.
516 11. Hahn MW, Höfle MG. 1998. Grazing pressure by a bacterivorous flagellate reverses
517 the relative abundance of *Comamonas acidovorans*PX54 and *Vibrio* Strain CB5 in
518 chemostat cocultures. Appl Environ Microbiol 64:1910-1918.
519 12. Hahn MW, Moore ER, Höfle MG. 1999. Bacterial filament formation, a defense
520 mechanism against flagellate grazing, is growth rate controlled in bacteria of different
521 phyla. Appl Environ Microbiol 65:25-35.
522 13. Wildschutte H, Wolfe DM, Tamewitz A, Lawrence JG. 2004. Protozoan predation,
523 diversifying selection, and the evolution of antigenic diversity in *Salmonella*.
524 Proceedings of the National Academy of Sciences, USA 101:10644-9.
525 14. Matz C, McDougald D, Moreno AM, Yung PY, Yildiz FH, Kjelleberg S. 2005.
526 Biofilm formation and phenotypic variation enhance predation-driven persistence of
527 *Vibrio cholerae*. Proceedings of the National Academy of Sciences, USA 102:16819-
528 24.
529 15. Jousset A. 2012. Ecological and evolutive implications of bacterial defences against
530 predators. Environ Microbiol 14:1830-43.
531 16. Chavez-Dozal A, Gorman C, Erken M, Steinberg PD, McDougald D, Nishiguchi MK.
532 2013. Predation response of *Vibrio fischeri* biofilms to bacterivorus protists. Appl
533 Environ Microbiol 79:553-8.

Downloaded from https://journals.asm.org/journal/aem on 01 December 2021 by 116.255.0.193.

Accepted Manuscript Posted Online

Applied and Environmental Microbiology

534 17. Matz C, Deines P, Boenigk J, Arndt H, Eberl L, Kjelleberg S, Jurgens K. 2004.
535 Impact of violacein-producing bacteria on survival and feeding of bacterivorous
536 nanoflagellates. Appl Environ Microbiol 70:1593-9.
537 18. Noorian P, Hu J, Chen Z, Kjelleberg S, Wilkins MR, Sun S, McDougald D. 2017.
538 Pyomelanin produced by *Vibrio cholerae* confers resistance to predation by
539 *Acanthamoeba castellanii*. FEMS Microbiol Ecol 93.
540 19. Sun S, Tay QX, Kjelleberg S, Rice SA, McDougald D. 2015. Quorum sensing-
541 regulated chitin metabolism provides grazing resistance to *Vibrio cholerae* biofilms.
542 ISME J 9:1812-20.
543 20. Lainhart W, Stolfa G, Koudelka GB. 2009. Shiga toxin as a bacterial defense against
544 a eukaryotic predator, *Tetrahymena thermophila*. J Bacteriol 191:5116-5122.
545 21. Pukatzki S, Ma AT, Sturtevant D, Krastins B, Sarracino D, Nelson WC, Heidelberg
546 JF, Mekalanos J. 2006. Identification of a conserved bacterial protein secretion
547 system in *Vibrio cholerae* using the *Dictyostelium* host model system. Proceedings of
548 the National Academy of Sciences, USA 103:1528-1533.
549 22. Pukatzki S, Ma AT, Revel AT, Sturtevant D, Mekalanos J. 2007. Type VI secretion
550 system translocates a phage tail spike-like protein into target cells where it cross-links
551 actin. Proceedings of the National Academy of Sciences, USA 104:15508-15513.
552 23. Miyata ST, Kitaoka M, Brooks TM, McAuley SB, Pukatzki S. 2011. *Vibrio cholerae*
553 requires the Type VI SecretionSystem virulence factor VasX to kill *Dictyostelium*
554 *discoideum*. Infect Immun 79:2941-2949.
555 24. Vaitkevicius K, Lindmark B, Ou G, Song T, Toma C, Iwanaga M, Zhu J, Andersson
556 A, Hammarström M-L, Tuck S. 2006. A *Vibrio cholerae* protease needed for killing
557 of *Caenorhabditis elegans* has a role in protection from natural predator grazing.
558 Proceedings of the National Academy of Sciences, USA 103:9280-9285.

Downloaded from https://journals.asm.org/journal/aem on 01 December 2021 by 116.255.0.193.

Accepted Manuscript Posted Online

Applied and Environmental Microbiology

AEM

Applied and Environmental Microbiology

559 25. Sun S, Kjelleberg S, McDougald D. 2013. Relative contributions of Vibrio
560 polysaccharide and quorum sensing to the resistance of *Vibrio cholerae* to predation
561 by heterotrophic protists. PLoS One 8:e56338.
562 26. Erken M, Weitere M, Kjelleberg S, McDougald D. 2011. In situ grazing resistance of
563 *Vibrio cholerae* in the marine environment. FEMS Microbiol Ecol 76:504-12.
564 27. Lee CT, Pajuelo D, Llorens A, Chen YH, Leiro JM, Padros F, Hor LI, Amaro C.
565 2013. MARTX of *Vibrio vulnificus* biotype 2 is a virulence and survival factor.
566 Environ Microbiol 15:419-32.
567 28. Kim BS. 2018. The Modes of Action of MARTX Toxin Effector Domains. Toxins
568 (Basel) 10:507.
569 29. Sambrook J, Fritsch EF, Maniatis T. 1989. Molecular cloning: a laboratory manual.
570 Cold Spring Harbor Laboratory Press.
571 30. Mårdén P, Tunlid A, Malmcrona-Friberg K, Odham G, Kjelleberg S. 1985.
572 Physiological and morphological changes during short term starvation of marine
573 bacterial islates. Arch Microbiol 142:326-332.
574 31. Väätänen P. 1977. Effects of Composition of Substrate and Inoculation Technique on
575 Plate Counts of Bacteria in the Northern Baltic Sea. J Appl Bacteriol 42:437-443.
576 32. Chen C, Khaleel SS, Huang H, Wu CH. 2014. Software for pre-processing Illumina
577 next-generation sequencing short read sequences. Source Code Biol Med 9:8.
578 33. Kopylova E, Noé L, Da Silva C, Berthelot J-F, Alberti A, Aury J-M, Touzet H. 2015.
579 Deciphering metatranscriptomic data, p 279-291, RNA Bioinformatics. Springer.
580 34. Noorian P, Sun S, McDougald D. 2018. Complete Genome Sequence of Oyster
581 Isolate *Vibrio vulnificus* Env1. Genome announcements 6:e00421-18.
582 35. Langmead B, Salzberg SL. 2012. Fast gapped-read alignment with Bowtie 2. Nat
583 Methods 9:357-9.

Downloaded from https://journals.asm.org/journal/aem on 01 December 2021 by 116.255.0.193.

Accepted Manuscript Posted Online
Applied and Environmental Microbiology
AEM
Applied and Environmental Microbiology

584 36. Anders S, Pyl PT, Huber W. 2015. HTSeq—a Python framework to work with high-
585 throughput sequencing data. Bioinformatics 31:166-169.
586 37. Love MI, Huber W, Anders S. 2014. Moderated estimation of fold change and
587 dispersion for RNA-seq data with DESeq2. Genome Biol 15:550.
588 38. Jayakumar JM, Shapiro OH, Almagro-Moreno S. 2020. Improved method for
589 transformation of Vibrio vulnificus by electroporation. Curr Protoc Microbiol
590 58:e106.
591 39. Clark DJ, Maaløe O. 1967. DNA replication and the division cycle in *Escherichia*
592 *coli*. J Mol Biol 23:99-112.
593 40. Wright AC, Simpson LM, Oliver JD. 1981. Role of iron in the pathogenesis of *Vibrio*
594 *vulnificus* infections. Infect Immun 34:503-7.
595 41. Yoon BK, Jackman JA, Valle-Gonzalez ER, Cho NJ. 2018. Antibacterial Free Fatty
596 Acids and Monoglycerides: Biological Activities, Experimental Testing, and
597 Therapeutic Applications. Int J Mol Sci 19:1114.
598 42. Wolfe AJ. 2005. The acetate switch. Microbiol Mol Biol Rev 69:12-50.
599 43. Minato Y, Fassio SR, Wolfe AJ, Hase CC. 2013. Central metabolism controls
600 transcription of a virulence gene regulator in *Vibrio cholerae*. Microbiology
601 (Reading) 159:792-802.
602 44. Ullah A, Orij R, Brul S, Smits GJ. 2012. Quantitative analysis of the modes of growth
603 inhibition by weak organic acids in *Saccharomyces cerevisiae*. Appl Environ
604 Microbiol 78:8377-87.
605 45. Jarboe LR, Royce LA, Liu P. 2013. Understanding biocatalyst inhibition by
606 carboxylic acids. Front Microbiol 4:272.

Downloaded from https://journals.asm.org/journal/aem on 01 December 2021 by 116.255.0.193.

Applied and Environmental Microbiology
AEM
Applied and Environmental Microbiology
Accepted Manuscript Posted Online

607 46. Gabba M, Frallicciardi J, van 't Klooster J, Henderson R, Syga L, Mans R, van Maris
608 AJA, Poolman B. 2020. Weak Acid Permeation in Synthetic Lipid Vesicles and
609 Across the Yeast Plasma Membrane. Biophys J 118:422-434.
610 47. Bamdad M, Groliere CA, Dupy-Blanc J, Cuer A, David L, Tabet JC. 1993. Microbial
611 conversion of lonophorous antibiotic nigericin by the ciliate *Tetrahymena pyriformis*.
612 Eur J Protistol 29:407-15.
613 48. Bamdad M, David L, Groliere CA. 1995. Epinigericin toxicity towards *Tetrahymena*
614 *pyriformis* GL; changes in cell volume and intracellular pH. Appl Microbiol
615 Biotechnol 44:206-9.
616 49. Ricke SC. 2003. Perspectives on the use of organic acids and short chain fatty acids as
617 antimicrobials. Poult Sci 82:632-9.
618 50. Desbois AP, Smith VJ. 2010. Antibacterial free fatty acids: activities, mechanisms of
619 action and biotechnological potential. Appl Microbiol Biotechnol 85:1629-42.
620 51. Kim CM, Park RY, Choi MH, Sun HY, Shin SH. 2007. Ferrophilic characteristics of
621 *Vibrio vulnificus* and potential usefulness of iron chelation therapy. J Infect Dis
622 195:90-8.
623 52. Gunsalus RP, Park SJ. 1994. Aerobic-anaerobic gene regulation in *Escherichia coli*:
624 control by the ArcAB and Fnr regulons. Res Microbiol 145:437-50.
625 53. Chang DE, Smalley DJ, Conway T. 2002. Gene expression profiling of *Escherichia*
626 *coli* growth transitions: an expanded stringent response model. Mol Microbiol 45:289-
627 306.
628 54. Vemuri GN, Altman E, Sangurdekar DP, Khodursky AB, Eiteman MA. 2006.
629 Overflow metabolism in *Escherichia coli* during steady-state growth: transcriptional
630 regulation and effect of the redox ratio. Appl Environ Microbiol 72:3653-61.

Downloaded from https://journals.asm.org/journal/aem on 01 December 2021 by 116.255.0.193.

Accepted Manuscript Posted Online

Applied and Environmental Microbiology

AEM

Applied and Environmental Microbiology

631 55. Basan M, Hui S, Williamson JR. 2017. ArcA overexpression induces fermentation
632 and results in enhanced growth rates of *E. coli*. Sci Rep 7:11866.

633 56. Szenk M, Dill KA, de Graff AMR. 2017. Why do fast-growing bacteria enter
634 overflow metabolism? Testing the membrane real estate hypothesis. Cell systems
635 5:95-104.

636 57. Wolfe AJ. 2008. Quorum sensing "flips" the acetate switch. J Bacteriol 190:5735-7.

637 58. Studer SV, Mandel MJ, Ruby EG. 2008. AinS quorum sensing regulates the *Vibrio*
638 *fischeri* acetate switch. J Bacteriol 190:5915-23.

639 59. Bueno E, Pinedo V, Cava F. 2020. Adaptation of *Vibrio cholerae* to Hypoxic
640 Environments. Front Microbiol 11:739.

641 60. Kim YR, Lee SE, Kim CM, Kim SY, Shin EK, Shin DH, Chung SS, Choy HE,
642 Progulske-Fox A, Hillman JD, Handfield M, Rhee JH. 2003. Characterization and
643 pathogenic significance of *Vibrio vulnificus* antigens preferentially expressed in
644 septicemic patients. Infect Immun 71:5461-71.

645 61. Poole MD, Oliver JD. 1978. Experimental pathogenicity and mortality in ligated ileal
646 loop studies of the newly reported halophilic lactose-positive *Vibrio* sp. Infect Immun
647 20:126-9.

648 62. Hayat U, Reddy GP, Bush CA, Johnson JA, Wright AC, Morris JG, Jr. 1993.
649 Capsular types of *Vibrio vulnificus*: an analysis of strains from clinical and
650 environmental sources. J Infect Dis 168:758-62.

651 63. Hor LI, Chang YK, Chang CC, Lei HY, Ou JT. 2000. Mechanism of high
652 susceptibility of iron-overloaded mouse to *Vibrio vulnificus* infection. Microbiol
653 Immunol 44:871-8.

654 64. Miyoshi N, Shimizu C, Miyoshi S, Shinoda S. 1987. Purification and characterization
655 of *Vibrio vulnificus* protease. Microbiol Immunol 31:13-25.

Downloaded from https://journals.asm.org/journal/aem on 01 December 2021 by 116.255.0.193.

656

Downloaded from https://journals.asm.org/journal/aem on 01 December 2021 by 116.255.0.193.

Applied and Environmental Microbiology
AEM
Applied and Environmental Microbiology
Accepted Manuscript Posted Online

Accepted Manuscript Posted Online

Applied and Environmental Microbiology

AEM

Applied and Environmental Microbiology

657 **List of Figures**

658 **Figure 1.** Percentage of bacterial survival (A) and number of *T. pyriformis* (B) after 24 h of
659 co-culture between different strains of *V. vulnificus* with *T. pyriformis.* The percentage of *V.*
660 *vulnificus* survival was quantified by measuring optical density of the co-culture ($OD_{600\ nm}$)
661 in relation to the control cells grown without *T. pyriformis* (100% survival) (A). The number
662 of *T. pyriformis* was determined from the co-culture by direct counts using an inverted
663 microscope under bright field illumination and compared with the cells cultured without
664 bacteria (B). Experiments were conducted with three replicate samples and repeated three
665 times separately. Error bars represent standard deviation. Statistical analysis was performed
666 using 2-way ANOVA and Sidak's multiple comparisons test (A) and 1-way ANOVA and
667 Dunnett's multiple comparisons test comparing all strains with the VNSS media control (B).
668 Statistical significance is indicated by *, p >0.05 cell density not different between ENV1
669 grown with or without T. pyriformis) (A), and NS, $P > 0.05$ (B).

670

Downloaded from https://journals.asm.org/journal/aem on 01 December 2021 by 116.255.0.193.

Accepted Manuscript Posted Online
AEM
Applied and Environmental Microbiology
Applied and Environmental Microbiology

671 **Figure 2.** Visualisation of *T. pyriformis* incubated in CFS of *V. vulnificus* ENV1 over 2 h.
672 Actively swimming cells (A) stopped swimming and sank to the bottom of the plate and cells
673 appear to leak cytoplasm after 1 h incubation (B). Complete lysis and degradation of cell
674 membranes was observed after 2 h (C). Scale bar = 100 µm.

Downloaded from https://journals.asm.org/journal/aem on 01 December 2021 by 116.255.0.193.

Accepted Manuscript Posted Online

675 **Figure 3.** Percentage of bacterial survival (A) and number of *T. pyriformis* (B) after 24 h of
676 co-culture of *V. vulnificus* ENV1 WT, ENV1 WT supplemented with 2-2' bipyridyl (BPD)
677 and *ΔarcA* mutant with *T. pyriformis*. Concentration of short chain fatty acids (acetate,
678 propionate, butyrate, and valerate) in the CFS of ENV1 after 24 hours of growth under
679 aerobic conditons at RT (C). Acetate excretion (D), growth at $OD_{600\ nm}$ (E) and pH (F) of *V.*
680 *vulnificus* ENV1 WT (filled circles), ENV1 WT supplemented with 2-2' bipyridyl (open
681 circles), and *ΔarcA* (filled rectangles). Growth was measued up to 7 h, and acetate
682 concentration and pH were measued up to 3 hours where growth was maximal. Experiments
683 were run in 0.5 × VNSS medium with at least 3 replicates. Error bars represent standard
684 deviation. Statistical analysis was performed using 2-way ANOVA and Sidak's multiple
685 comparisons test (A) and 1-way ANOVA and Dunnett's multiple comparisons test comparing
686 all strains with the VNSS media control (B). * $p < 0.05$.

Downloaded from https://journals.asm.org/journal/aem on 01 December 2021 by 116.255.0.193.

Accepted Manuscript Posted Online

687

688 **Figure 4**. A model based on the genes that are upregulated under iron replete conditions
689 describing the overflow metabolism that enables synthesis and excretion of acetate by *V.*
690 *vulnificus* ENV1, based on the RNA sequence analysis (Table 3). The master regulator, *arcA,*
691 represses the TCA cycle and as a result the acetyl-CoA is diverted to the *pta-ackA* pathway
692 and leads to excretion of acetate. g*pi;* glucose-6-phosphate, *pfkA;* phosphofructokinase, *tpiA;*
693 triosephosphate isomerase, *gpmI;* phosphoglycerate mutase, *eno;* enolase, *pyk*; pyruvate
694 kinase, *arcA;* Anaerobic regulator, *pfl*; pyruvate-formate lyase, *fdhA*; formate dehydrogenase,
695 *ackA;* acetate kinase, aldh; acetaldehyde dehydrogenase*, adh;* alcohol dehydrogenase.

696

697

Downloaded from https://journals.asm.org/journal/aem on 01 December 2021 by 116.255.0.193.

Accepted Manuscript Posted Online

Applied and Environmental Microbiology

AEM

Applied and Environmental Microbiology

698 **Figure 5.** Acetate excretion (A), growth at $OD_{600\ nm}$ (B), and pH (C) of *V. vulnificus* strains

699 ENV1 (filled circles) and the grazing sensitive L180 (empty squares), under aerobic

700 conditions.

Downloaded from https://journals.asm.org/journal/aem on 01 December 2021 by 116.255.0.193.

Accepted Manuscript Posted Online

Applied and Environmental Microbiology

AEM

Applied and Environmental Microbiology

701 **List of Tables**

702 **Table 1.** List of bacterial and protozoal strains.

Strain	Properties	Source*	Reference
Bacteria			
CMCP6	C-genotype, clinical isolate, WT	Human blood Korea	(60)
C7184	C-genotype, clinical isolate, WT	Human blood Atlanta	(61)
MO6-24	C-genotype, clinical isolate, WT	Human blood California	(62)
YJ016	C-genotype, clinical isolate, WT	Human blood Taiwan	(63)
L-180	C-genotype, clinical isolate, WT	Human blood Japan	(64)
JY1701	E-genotype, environmental isolate, WT	Oyster Louisiana	(3)
JY1305	E-genotype, environmental isolate, WT	Oyster Louisiana	(3)
ENV1	E-genotype, environmental isolate, WT	Oyster Louisiana	(3)
SS108-A3A	E-genotype, environmental isolate, WT	Oyster Louisiana	(3)

Downloaded from https://journals.asm.org/journal/aem on 01 December 2021 by 116.255.0.193.

Accepted Manuscript Posted Online
Applied and Environmental Microbiology
AEM
Applied and Environmental Microbiology

LSU2098	E-genotype, clinical isolate, WT	Human Wound *Nk	(3)
LSU549	E-genotype, clinical isolate, WT	Human Wound *Nk	(3)
LSU1657	E-genotype, clinical isolate, WT	Human Wound *Nk	(3)
E64MW	E-genotype, clinical isolate, WT	Human Wound *Nk	(3)
Protozoa			
T. pyriformis	Wild type		ATCC 205063
U. marinum (Dujardin 1841)	Wild type		Isolated by Dr Martina Erken (2011, Sydney Institute of Marine Science)

703 *NK = Not known

Downloaded from https://journals.asm.org/journal/aem on 01 December 2021 by 116.255.0.193.

Accepted Manuscript Posted Online
Applied and Environmental Microbiology
AEM
Applied and Environmental Microbiology

704 **Table 2.** Survival of *T. pyriformis* when exposed to CFS from *V. vulnificus* ENV1 and 0.5 ×
705 VNSS medium with and without the physical and chemical treatments for 2 h.

CFS / Media / Treatment	**pH^**	***T. pyriformis* survival#**
ENV1 CFS	4.6	Dead
Heat treatment (2hours-95 °C)	4.6	Dead
Freeze/ Thaw (-20 °C)	4.6	Dead
Ultrafiltration (Amicon® Ultra-0.5-10,000 NMWL)	4.6	Dead
Protease	4.6	Dead
Proteinase K	4.6	Dead
NaOH	7.0	Alive
CFS of ENV1 grown under iron-deplete conditions	5.1	Alive
0.5 X VNSS	7.4	Alive
1 mM HCl	6.0	Alive
2 mM HCl	4.5	Alive
3 mM HCl	3.8	Alive
1 mM Acetic acid	5.5	Alive
2 mM Acetic acid	4.8	Alive
3 mM Acetic acid	4.5	Dead
1 mM Acetic acid + HCl	3.9	Dead
2 mM Acetic acid + HCl	3.8	Dead

707 #*T. pyriformis* cell suspension was considered dead when less than 10% of the cells were
708 active and alive when more than 90% of the cells were active, compared to the total active
709 cells in the untreated control.

Downloaded from https://journals.asm.org/journal/aem on 01 December 2021 by 116.255.0.193.

Applied and Environmental Microbiology
AEM
Applied and Environmental Microbiology
Accepted Manuscript Posted Online

710 ^ Values are ± 0.05.

Downloaded from https://journals.asm.org/journal/aem on 01 December 2021 by 116.255.0.193.

Accepted Manuscript Posted Online
Applied and Environmental Microbiology
AEM
Applied and Environmental Microbiology

711 **Table 3**. Differential expression of genes involved in glycolysis, the repression of 712 tricarboxylic acid cycle (TCA), pyruvate fermentation, acetate excretion, and other oxidised 713 metabolites. Complete list of all differentially expressed genes are provided in the 714 supplementary information (Table S1).

Gene locus ID	Expression fold change (log2)	Adjusted p-value	Gene annotation	Function
Glycolysis, Glucose to Pyruvate				
BJD94_12875	1.9217	2.125E-08	Glucose-6-phosphate isomerase, *gpi*	glucose-6-phosphate to fructose-6-phosphate
BJD94_12175	1.8042	2.374E-07	6-phosphofructokinase, *pfkA*	fructose 6-phosphate to fructose 1,6-bisphosphate
BJD94_12630	1.379	1.121E-07	Triosephosphate isomerase, *tpiA*	dihydroxyacetone phosphate (DHAP) to D-glyceraldehyde-3-phosphate (G3P)
BJD94_12290	1.3784	6.156E-10	22C3-bisphosphoglycerate-independent phosphoglycerate	2-phosphoglycerate (2-PGA) and 3-phosphoglycerate (3-PGA)

Downloaded from https://journals.asm.org/journal/aem on 01 December 2021 by 116.255.0.193.

Accepted Manuscript Posted Online
Applied and Environmental Microbiology
AEM
Applied and Environmental Microbiology

			mutase, *gpmI*	
BJD94_13755	1.345	0.0002797	Enolase, *eno*	2-PGA to Phosphoenolpyruvate
BJD94_09310	1.2669	0.0011528	Pyruvate kinase, *pyk*	Phosphoenolpyruvate to pyruvate
Pyruvate fermentation to Acetyl-CoA				
BJD94_14015	-1.7379	0.3487340 9	Dihydrolipoamide dehydrogenase of pyruvate dehydrogenase complex, *pdhC*	Aerobic decarboxylation of Pyruvate to Acetyl-CoA
BJD94_08715	3.8163	3.65E-108	Pyruvate formate-lyase, *tdcE* or *grcA*	Pyruvate to acetyl CoA and formate
BJD94_01215	4.2489	0	Pyruvate formate-lyase, *pfl*	Pyruvate to acetyl CoA and formate
Formate dehydrogenation to CO2				
BJD94_18845	1.922	0.0009791	NAD-dependent formate dehydrogenase alpha subunit, *fdhA*	formate to CO2
Repression of tricarboxylic acid (TCA) cycle				
BJD94_00805	1.9081	0.0005814	Phosphohistidine	Regulation of

Downloaded from https://journals.asm.org/journal/aem on 01 December 2021 by 116.255.0.193.

Accepted Manuscript Posted Online

Applied and Environmental Microbiology

AEM

Applied and Environmental Microbiology

			phosphatase, *SixA*	arcB/arcA two component system
BJD94_08750	1.8356	2.715E-08	Anaerobic aerobic respiration control protein, arcA	Represses TCA cycle
Acetate metabolism				
BJD94_01780	1.5263	4.2E-06	Acetate kinase, *ackA*	Acetyl-CoA to Acetate
BJD94_20925	2.391	0.0314181	Acetate kinase, *ackA*	Acetyl-CoA to Acetate
BJD94_06220	1.6943	1.142E-36	Alcohol dehydrogenase 3B Acetaldehyde dehydrogenase, *adh/aldh*	Acetyl-CoA to Ethanol to acetaldehyde to Acetate

715

716

717

Downloaded from https://journals.asm.org/journal/aem on 01 December 2021 by 116.255.0.193.

Accepted Manuscript Posted Online

Applied and Environmental Microbiology

AEM

Applied and Environmental Microbiology

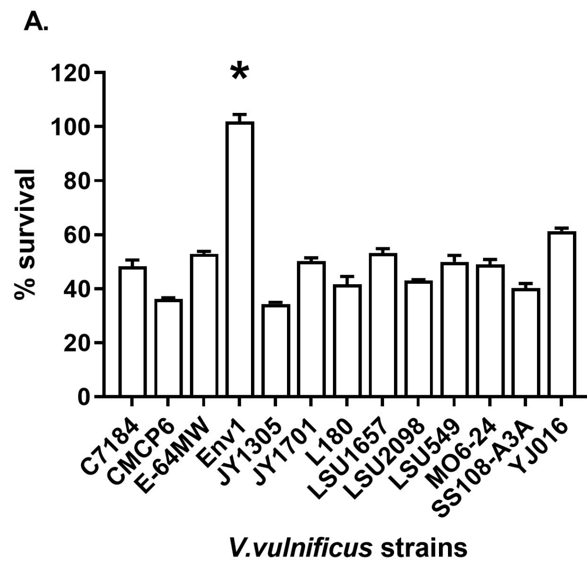

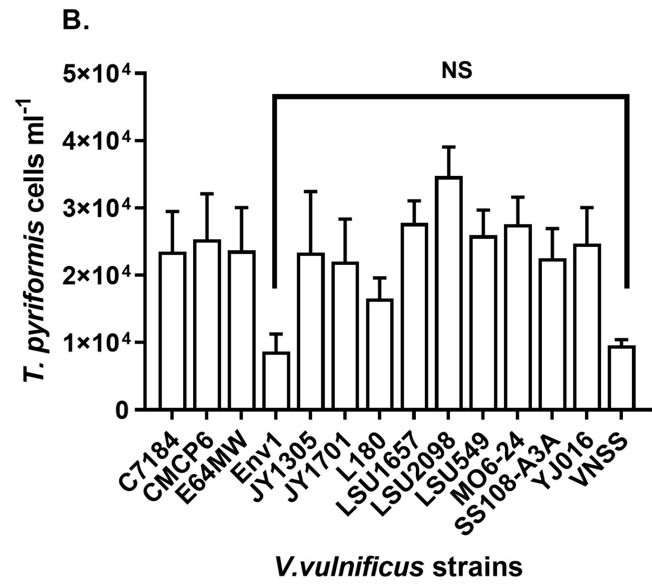

Downloaded from https://journals.asm.org/journal/aem on 01 December 2021 by 116.255.0.193.

Accepted Manuscript Posted Online
Applied and Environmental Microbiology
AEM
Applied and Environmental Microbiology

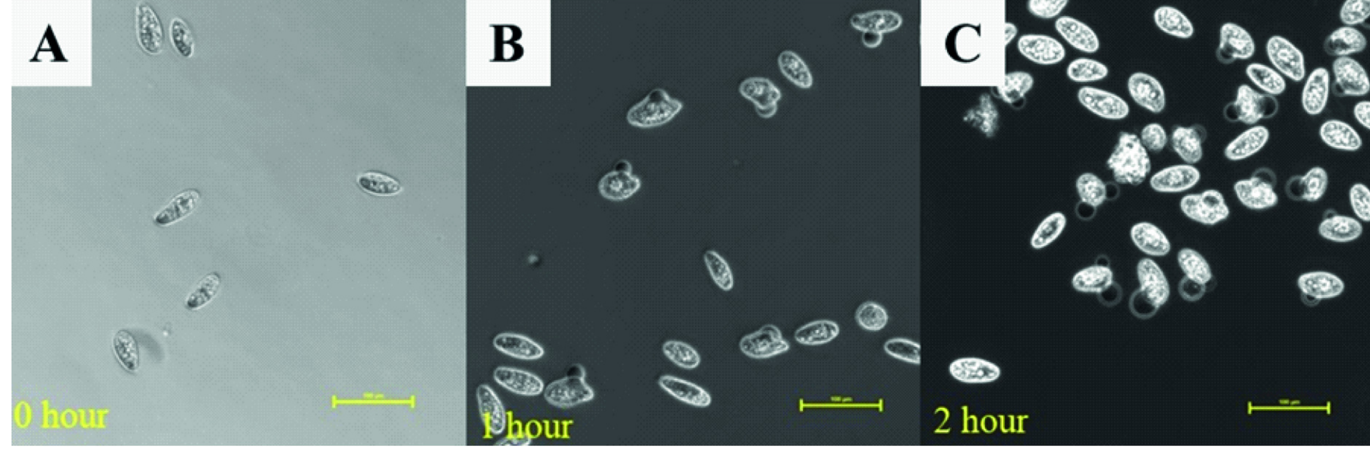

Downloaded from https://journals.asm.org/journal/aem on 01 December 2021 by 116.255.0.193.

Accepted Manuscript Posted Online

Applied and Environmental Microbiology

AEM

Applied and Environmental Microbiology

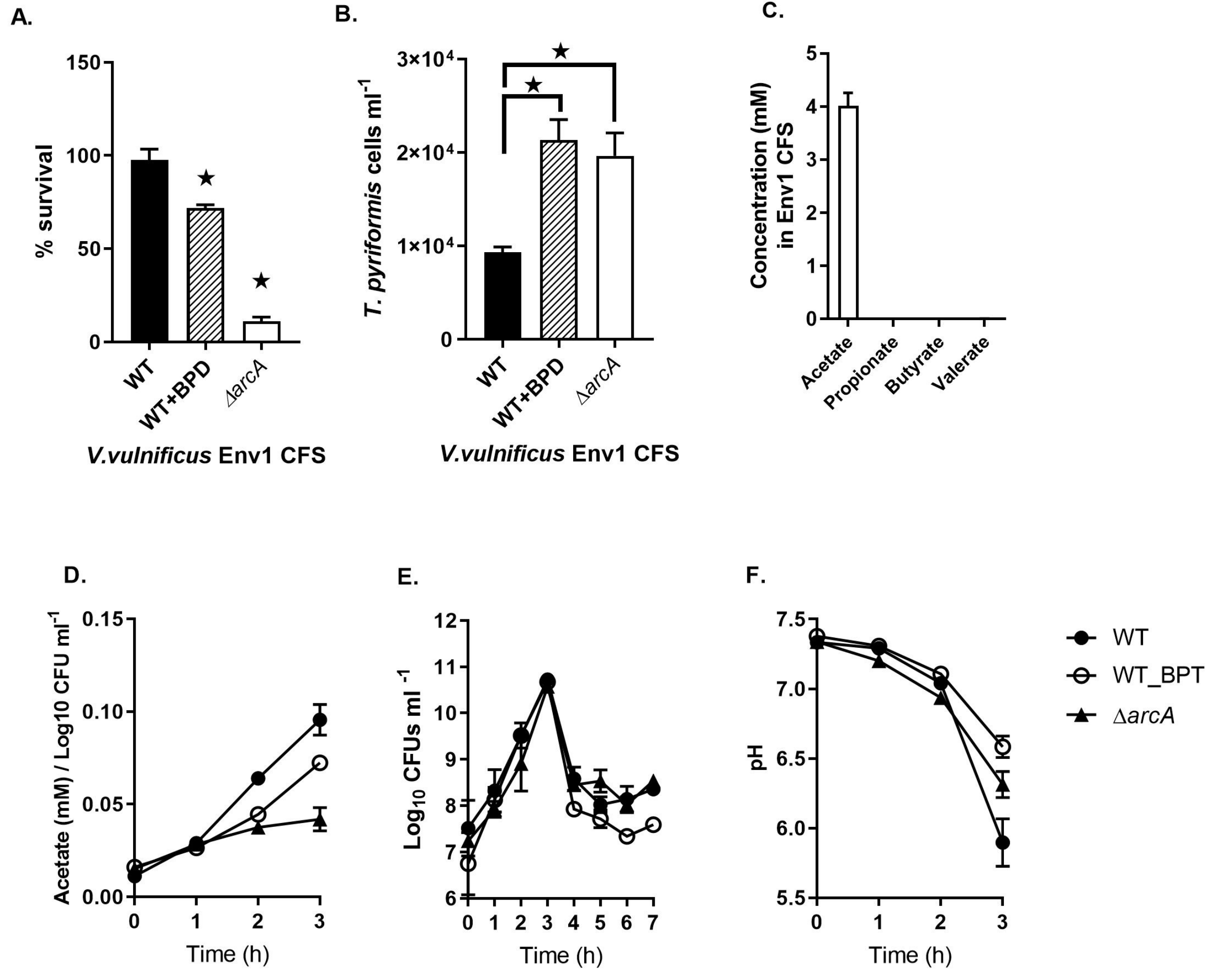

Downloaded from https://journals.asm.org/journal/aem on 01 December 2021 by 116.255.0.193.

Accepted Manuscript Posted Online
Applied and Environmental Microbiology
AEM
Applied and Environmental Microbiology

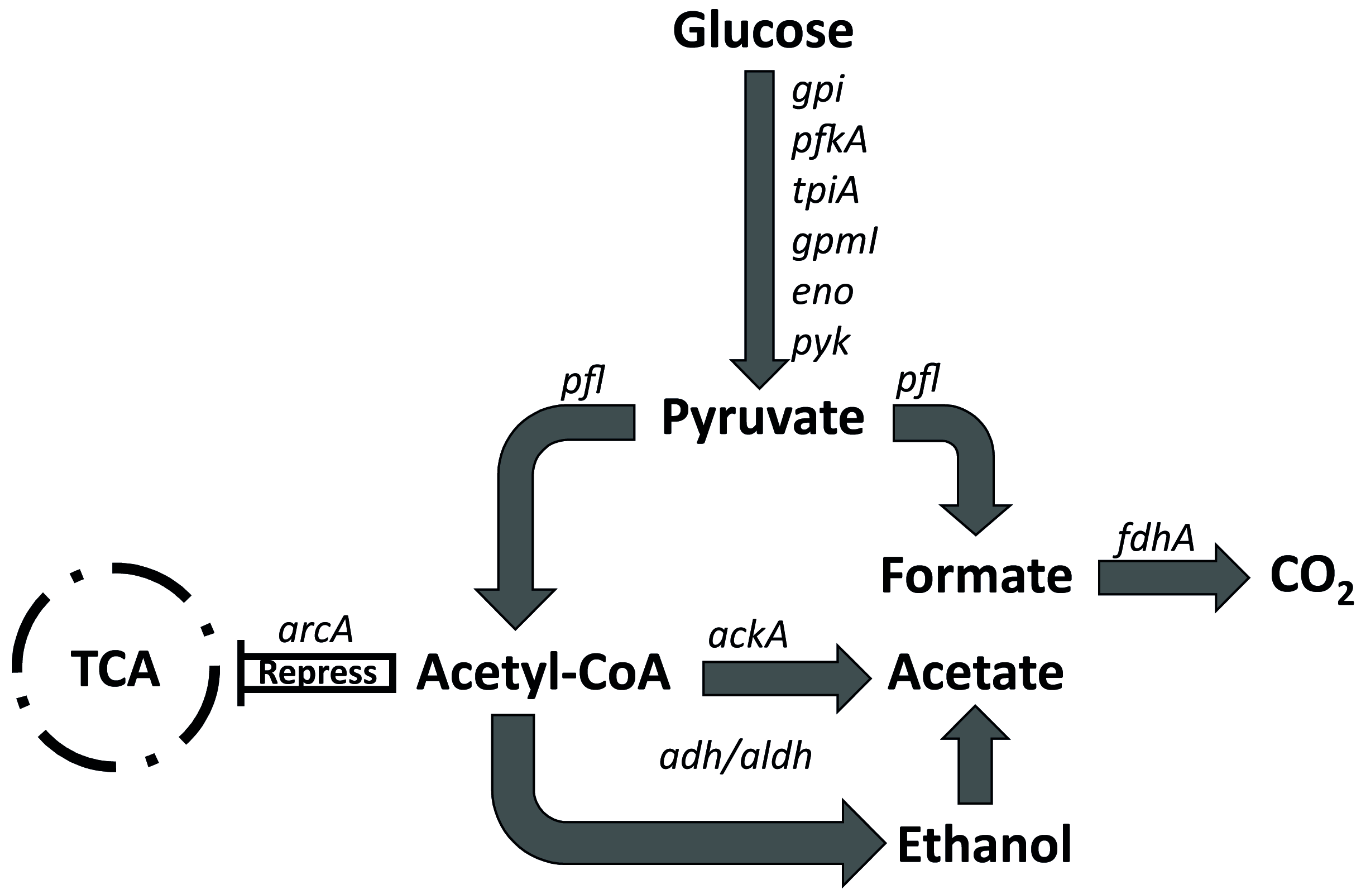

Downloaded from https://journals.asm.org/journal/aem on 01 December 2021 by 116.255.0.193.

Accepted Manuscript Posted Online
Applied and Environmental Microbiology
AEM
Applied and Environmental Microbiology

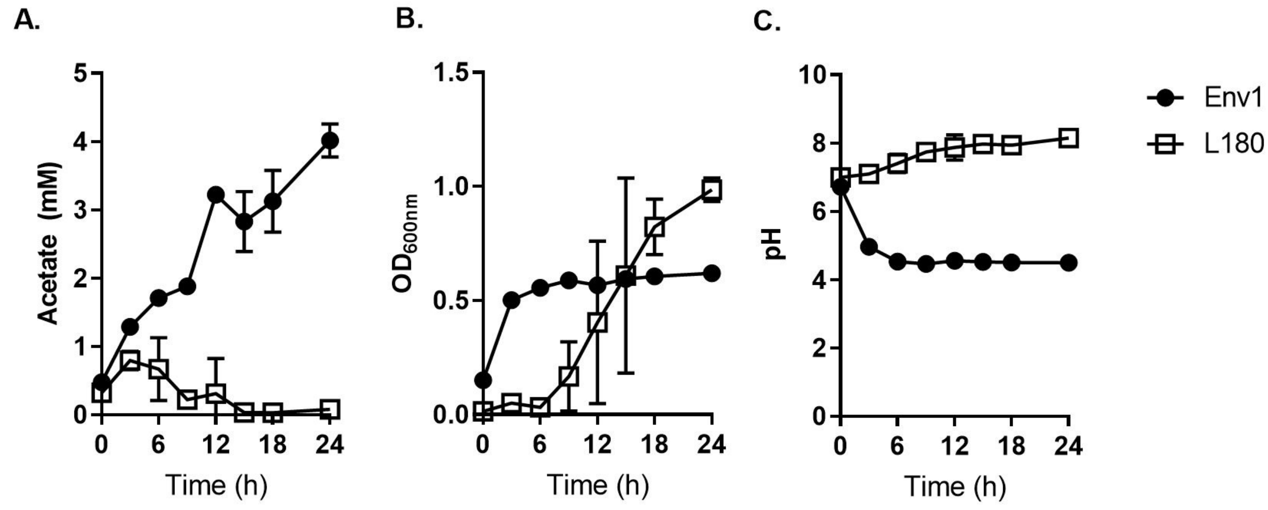

Downloaded from https://journals.asm.org/journal/aem on 01 December 2021 by 116.255.0.193.